24th COBEM - 2017

24th ABCM International Congress of Mechanical Engineering
December 3-8, 2017, Curitiba, PR, Brazil

COBEM-2017-0369
EVALUATION OF THE CONSEQUENCES OF FREE FALLING LOADS IN POLYESTER YARNS

Emilio Luiz Vieira Louzada
Carlos Eduardo Marcos Guilherme
Federal University of Rio Grande, Av. Italia, km. 8, Rio Grande, Brazil
emilioluizlouzada@gmail.com
carlosguilherme@furg.br

Felipe Tempel Stumpf
Federal University of Rio Grande do Sul - Department of Mechanical Engineering, Rua Sarmento Leite, 425, Porto Alegre, Brazil
felipe.stumpf@ufrgs.br

Abstract. *The increasing number of research regarding mooring systems promoted changes in the offshore industry, such as the replacement of steel cables by synthetic ropes, and the development of new types of anchors. In 2004 Petrobras designed the torpedo pile. The procedure of inserting the anchor to the seabed is a consequence of a free fall mechanism, however, during the installation of the torpedo anchor, an unexpected stop of the launching system might happen, causing an impact load to the synthetic anchoring cables. The synthetic cables are also used for other activities, such as towage, fire service escape, climbing and sailing sports, and might eventually be submitted to abrupt axial loads. Mainly for climbing sports, the polymeric ropes are an important equipment to protect the climber in a fall situation. Addressing these issues, this work aims to assess mechanical behavior of polyester (PET) ropes, produced by manufacturers A, B and C, when submitted to impact tensile stress, analyzing their fatigue life after the occurrence of an impact load.*

Keywords: *offshore industry, synthetic ropes, impact load*

1. INTRODUCTION

The close relation between Men and Materials is straightly connected to some periods registered on earth, like the Stone Age, Copper Age, Bronze Age, Iron Age and Steel Age, which names were given in order to represent the man's need of those materials in each period (Hage, 1998). Recently, the appearance of the polymers as an alternative to replace traditional materials (metal and ceramic) is causing a significant growth in the number of professionals working in this area (Hage, 1998).

Some polymeric materials are found in nature, such as natural rubber and cellulose, and only by the beginning of the twentieth century they were developed in the synthetic form, mainly because of the high compression of its molecular structure. Among the group of materials firstly synthesized, the Nylon® 66 stood out for replacing the natural fibers used by soldiers for climbing mountains during the Second World War due to its good mechanical performance (Mckenna *el al.*, 2004; Smith, 1998). Later, other polymers used by the rope manufacturers emerged, such as: polyester (PET), aramid, high modulus polyethylene (HMPE), and Kevlar® (Mckenna *et al.*, 2004).

Nowadays, the synthetic fibers are found in ropes used, for example, in the mooring of offshore platforms, ship towage operations, fire services escape, climbing sports and sailing related activities. Regarding the mooring of offshore platforms, the "Taut Leg" geometry stands out, in which the anchoring line is subdued to cyclical strains (da Costa Mattos and Chimisso, 2011; Louzada *et al.*, 2016; Wang *et al.*, 2016). In ship towage operations, the synthetic fibers are susceptible to hydrodynamics and/or inertial forces (Wang *et al*, 2008). During climbing sports and fire services scape, these ropes are important safety equipments that protect climbers and firefighters in eventual fall situations, reducing the impact forces transmitted to their bodies and, consequently, diminishing the risks of death or severe injuries (Martin *et al.*, 2014; Pavier, 1998; Vogwell and Minguez, 2007). Finally, in sailing related activities, the ropes are responsible for controlling the sail of the sailboat. As a result, they are submitted to different loadings (static or dynamic), because of the wind force (Mclaren, 2006).

Considering the above, the investigation of the mechanical properties of synthetic fibers in different conditions became a challenge for the engineers. The service conditions include different load cycles, temperature, humidity,

frequency, etc. These mechanical properties are evaluated by standard testing procedures that measure different parameters, such as strength, stiffness, elongation, among others (Nikonov *et al.*, 2011).

The purposes of this paper is to evaluate the tensile strength of polymeric multifilament submitted to dynamic forces, more specifically, cyclic and sudden loadings. This evaluation will be made by comparing the fatigue life of virgin PET yarns to a set of samples previously submitted to a free falling test. Furthermore, variables such as viscoplastic and maximum elongation will be measured during the tests. The conditions of the experiments are discussed based on BS EN 892:2012 standard, which is particularly related to polymeric ropes used in climbing activities.

2. DYNAMIC LOADINGS

As for the sudden loading investigation, Emri *et al.* (2008) supports that one alternative for the rope's behavior analysis is through an Experimental-Numerical-Analytic (ENA) methodology. This methodology evaluates the polymeric ropes by quantifying some physical parameters, such as maximum force, elastic deformation, viscoplastic deformation, maximum elongation, stored energy, dissipated energy and retrieved energy.

Concerning the experimental tests, they are similar to the ones from BS EN 892:2012 standard, which sets the parameters for the impact experiments on climbing ropes, basically consisting in a free falling mass (Fig. 1). The entry data are: rope length (l_0), free falling height (h), mass (m), and gravitational acceleration (g), along with standard atmospheric condition to commissioning and tests (temperature and relative humidity), which may directly interfere on the material's behaviour (Emri *et al*., 2008; Nikonov *et al.*, 2011; Vogwell and Minguez, 2007). It is important to highlight that several procedures are presented by this standard, depending on the investigated elements (stiffness, number of tests that the rope can handle before breaking, strength transmitted through the rope and maximum elongation), but it fails when it comes to presenting ways of measuring the rope's deformation through time, limiting the understanding of its behavior (Emri *et al*., 2008).

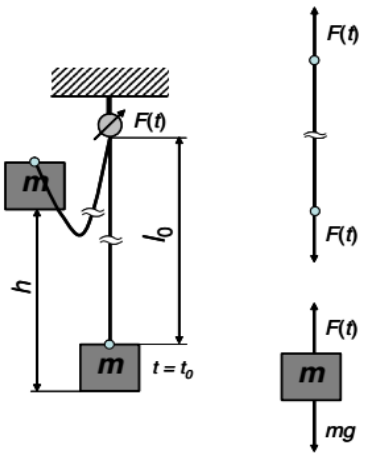

Figure 1. Schematics of a rope exposed to the impact test (Emri et al., 2008).

Regarding the analytical procedure, it is based on the free falling experiment shown in Fig. 1. A more detailed procedure is available in Emri et al. (2008). It is important to highlight that the results found in the analytical equations from the referred literature were considered suitable. Analyzing the experiment, while the mass is released from an arbitrary height ($h \leq l_0$) it is possible to measure the force in the time function F(t) on the upper anchorage of the rope (Fig. 1), and consequently establish the force transmitted through the rope and acting on the mass (Emri et al., 2008). Then, the force versus time curve (Fig. 2) is basically divided into three parts: A, B and C. The first part is represented by the mass in a free falling movement, performing a null loading until the rope is totally straightened in $t=t_0=\sqrt{2h/g}$ and its velocity equal to $v_0=\sqrt{2gh}$. Subsequently, still on T_0, part B is initiated. This step is characterized by the rope's deformation process and occurs between T_0 and T_7. Finally, between T_7 and T_9, part C takes place. In this step, the rope's loading becomes zero again and the mass starts to perform a free and upward vertical movement. Following, a second loading cycle is started if there is one, in which the analysis made is identical to the already mentioned (Emri *et al*., 2008; Nikonov *et al.*, 2011).

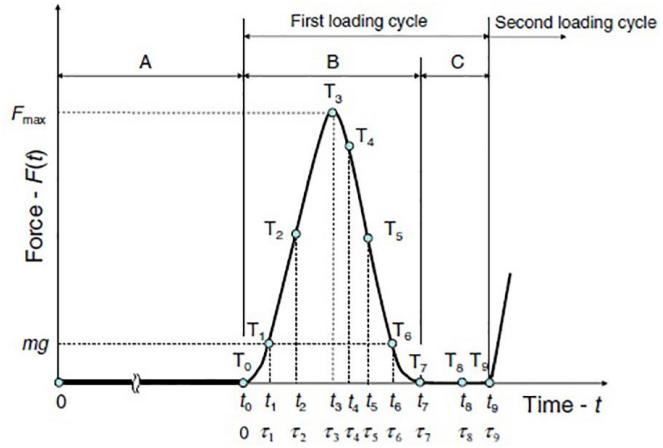

Figure 2. Schematics of the force measured during the impact test (Emri et al., 2008)

Analyzing step B, the mass movement equation is described below, neglecting the air resistance.

$$m\ddot{s}(\tau)=mg-F(\tau) \tag{1}$$

In Equation (1), m is equal to the mass, g is the gravitational acceleration and $\ddot{s}(\tau)$ is the second derivative of the mass displacement with respect to time. Applying the initial conditions from part B, $s(\tau=0)=0$ e $\dot{s}(\tau=0)=v_0=\sqrt{2gh}$ in Eq. (1), it is observed the viscoplastic and viscoelastic deformation equation of the rope (Eq. 2).

$$s(\tau)=\frac{g\tau^2}{2}-\frac{1}{m}\int_0^{\tau} F(\tau)\,d\tau+v_0\tau \tag{2}$$

From Equation (2), it is possible to obtain the velocity expression, acceleration/deceleration and the jolt (acceleration/deceleration rate) acting on the weight, respectively:

$$v(\tau)=\dot{s}(\tau)=g\tau-\frac{1}{m}\int_0^{\tau} F(\tau)d\tau+v_0 \tag{3}$$

$$a(\tau)=\ddot{s}(\tau)=g-\frac{F(\tau)}{m} \tag{4}$$

$$j=\dddot{s}(\tau)=\frac{1}{m}\frac{dF(\tau)}{d\tau} \tag{5}$$

Additionally, when replacing the expression of the Force-Time curve on Eq. (2), it is possible to find the force versus strain curve (Fig 3).

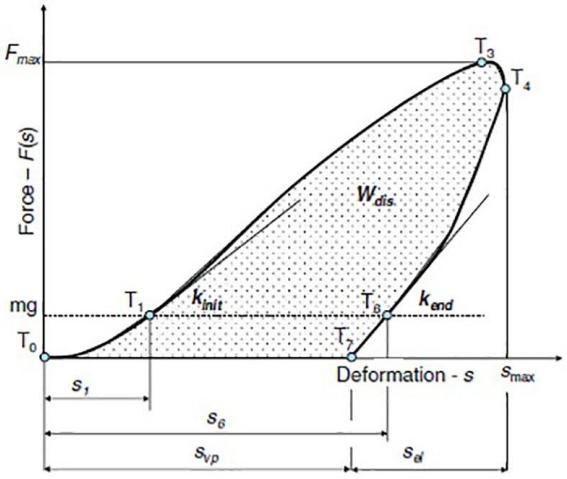

Figure 3. Force versus strain diagram of the rope submitted to the free falling test. (s_{max}) maximum deformation; (s_{vp}) viscoplastic deformation; (s_{el}) elastic deformation; (k_{init}) initial stiffness; (k_{end}) final stiffness; (W_{diss}) dissipated energy (Emri et al., 2008)

The materials behavior is described through time in part B. At T_1, the force acting on the rope is equal to $F(\tau_1) = mg$ and the mass is known for presenting the maximum velocity. At T_2 the deceleration rate will reach its extreme value. At T_3, the forces working on the rope and on the mass reach their highest values. Then, the rope has reached its maximum elongation, and consequently, the velocity of the dead weight becomes goes to zero. Because of the viscoelasticity of polymeric materials, the maximum force point does not match with the maximum elongation point (Fig. 4). From T_4 on, the rope's unloading is started, and it goes through the end of part B. Also at this point, the mass is accelerated in the opposite direction of the movement, because of the elastic component of the rope. At T_5, the acceleration rate will reach its extreme value, and after that, at T_6, the force acting on the rope becomes equal to the weight force again (Emri *et al*., 2008; Nikonov *et al.*, 2011).

Regarding the deformations, through Eq. (2) it is possible to find the maximum and viscoplastic components of the material and, consequently, the elastic deformation, respectively:

$$s_{max} = s(\tau_4) = \frac{g(\tau_4^2)}{2} - \frac{1}{m}\int_0^{\tau_4} F(\tau)d\tau + v_0(\tau_4) \tag{6}$$

$$s_{vp} = s(\tau_7) = \frac{g(\tau_7^2)}{2} - \frac{1}{m}\int_0^{\tau_7} F(\tau)d\tau + v_0(\tau_7) \tag{7}$$

$$s_{el} = s(\tau_4) - s(\tau_7) = s_{max} - s_{vp} \tag{8}$$

Besides the parameters that have already been mentioned, there are others such as stored energy, retrieved energy and, mainly, the dissipated energy that are also used to set the quality of the ropes (Emri *et al*., 2008; Nikonov *et al*., 2011). These parameters can be found on the rope's deformation energy equation through time, being it the same as the sum of the kinetic (W_k) and potential (W_{pt}) energies of the mass on the chosen moment, as shown in Eq. (9).

$$W(\tau) = W_k(\tau) + W_{pt}(\tau) \tag{9}$$

According to Emri *et al*. (2008) and Nikonov *et al*. (2011), combining the force curve versus the strain from T_0 to T_4, it is possible to find what we call stored energy (W_{store}) by the material, as in Eq. (10). This energy is equivalent to the total potential energy of the mass. The stored energy is the only source of energy absorption during the loading cycle (Emri et al., 2008).

$$W_{store} = \overbrace{mg\,(h + s_{max})}^{total\ potencial\ energy} \tag{10}$$

Concerning the rope's dissipated energy, element that straightly influences on the impact force transmitted to the mass, it can be found through the combination of the T_0 and T_7 points, or by the subtraction between stored and retrieved energies. The last one being related to the material's elasticity, boosting the mass upwards at $\tau_4$moment, and consequently not being a desirable characteristic for the rope. It is important to highlight that the thermal elements are not considered on the equations shown so far (Custer, 2006; Emri *et al*., 2008; Nikonov *et al*., 2011).

In terms of fatigue behavior, it is a phenomenon characterized by long term cyclic and static loadings, and its occurrence depends on variables such as geometry, loading type, rate and range, frequency, temperature, humidity and environmental pH (de Camargo *et al*., 2016; Mckenna *et al.*, 2004). However, it is impracticable to reproduce fatigue tests in the laboratory using the real offshore operating conditions, since PET ropes are designed to a 20 years minimum lifetime, so the bibliography addresses alternative tests that use higher amplitude or average load (Banfield et al.,1999).

3. MATERIALS AND METHODS

Synthetic ropes are composed of two components (mantle and core). The mantle is characterized by protecting the core from environmental damage and external abrasion. However, the core is responsible for the mechanical properties of the rope, such as tensile strength, fatigue and impact resistance (Banfield et al., 1999; Mclaren, 2006), so the core is the component to be studied in the present work.

The choice of the most suitable geometry to be used in the tests is based on the nominal capacity of the load cells of the testing machines, material availability and the cost of the component (sub-rope, leg, multifilaments and yarn) that form the core. Therefore, the scale of the multifilaments is considered the ideal for the progress of this research. Regarding the materials, PET from different brands are used and for confidentiality reasons they will be treated as PET A, PET B and PET C.

The test conditions are 500 mm long specimens with "sandwich" type terminations due to its good performance in previous tests (Pfarrius et al., 2007). These specimens are kept for at least 2 hours in a controlled environment with temperature of 20 ± 2°C and relative humidity of 65 ± 4%, before and during the tests, as the same conditions as recommended by ISO 139, which addresses the standard atmosphere for fiber conditioning and testing.

First, the tensile strength for each material (Tab. 1) was obtained on an INSTRON 3365 testing machine under the already mentioned testing conditions using a controlled ramp speed until rupture (ASTM D885: 1998). Each material had 30 specimens tested. It was found that PET A, PET B and PET C have tensile strength of 165,44 N, 171,71 N and 268,35 N, respectively.

Afterwards, a virgin sample was subjected to fatigue tests on an INSTRON 8810 testing machine using a cycling frequency of 0.1 Hz and loads ranging according to: 10 to 90% YBL, 20 to 90% YBL, 30 to 90% YBL, 40 to 90% YBL, 50 to 90% YBL, 60 to 90% YBL and 70 to 90% YBL, where YBL refers to the Yarn Break Load of the material. Twenty specimens were tested at each cyclic loading interval, which means a total of 140 multifilament for each material. The next step was to verify fatigue life when the specimen is previously subjected to an impact test on a testing device (Fig. 4) which provides the multifilament with a gravitational potential energy equivalent to a mass of 9% YBL released from a height equal to 300 mm. This procedure is performed for PET A, PET B and PET C. Barbetta et al. (2004) and Maroco (2007) suggest that a variance analysis to be performed to investigate the effect of material and impact load factors on the number of cycles until rupture. The confidence level used in the analysis is equal to 95%.

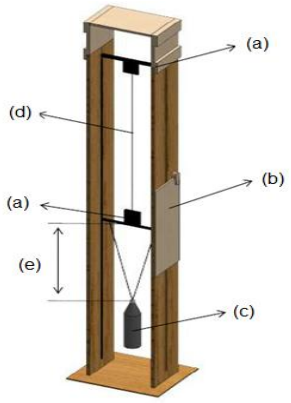

Figure 4. Free falling testing device. (a) terminals; (b) scale; (c) dead weight; (d) specimen; (e) height

4. RESULTS AND DISCUSSION

4.1 Effect of material and the impact testing on the fatigue life of polyester yarns

The results for the fatigue life of PET produced by manufacturer A and B, for the virgin materials, and for the specimens submitted to an impact load equivalent a mass of 9%YBL falling from a 300 mm of height, is disposed in Fig. 5.

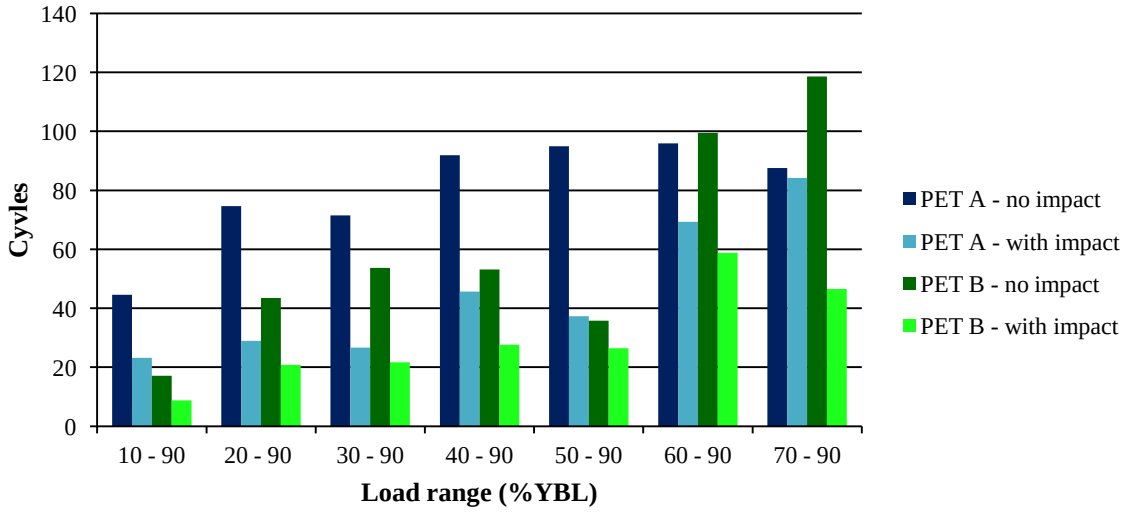

Figure 5. Diagram of the average number of cycles until rupture in each load range

In Figure 5, the virgin samples showed longer fatigue life than those previously subjected to a free fall test. Analyzing the “PET A samples - without impact” and “PET B - without impact”, a higher fatigue strength is observed for PET A when the lower load is equal to 10% YBL, 20% YBL, 30% YBL, 40% YBL and 50% YBL, and the higher

fatigue strength of the virgin PET 2 in the cyclic loads of 60% YBL at 90% YBL characterizes the good performance of this material at lower amplitudes. Comparing “PET A - with impact” versus “PET B - with impact”, it is possible to verify that in all tests PET A has lasted a larger number of cycles until rupture.

However, the average number of cycles up to the failure will may produce precipitous conclusions about the set of data, so it necessary to use a statistical test. Therefore, the diagram of average number of cycles until rupture in each load range (Fig. 6) was used to complement and to consolidate the results obtained in the analysis of variance that tests the influence of factors, material and impact load, on the fatigue life of the PETs. This statistical test doesn't predict the average reduction in the fatigue life of the polyester ropes in the real offshore operating conditions, if they are previously submitted to an impact load.

Analyzing the set of data through analysis of variance, were found evidence that the average number of cycles until rupture, both for virgin and previously submitted to an impact test, is higher in PET A than in PET B in cyclic loads from: 10 to 90% YBL, 20 to 90% YBL, 30 to 90% YBL, 40 to 90% YBL and 50 to 90% YBL. In addition, there are evidences that an impact load due to a free falling load of a mass equal to 9% YBL from a height of 300 mm is sufficient to cause a reduction of the fatigue resistance of multifilaments of PET A and PET B, in cyclic loads from: 10 to 90% YBL, 20 to 90% YBL, 30 to 90% YBL, 40 to 90% YBL, 50 to 90% YBL. Regarding PET C, it was observed in the tests that a mass equal to 9% YBL is sufficient to cause failure during the impact test on the multifilament.

In Figures 6 and 7, the trend curves are shown for different samples of PET A and PET B (both virgin and damaged by the impact test). The highlighted points represent the average number of cycles (log N) versus loading amplitude.

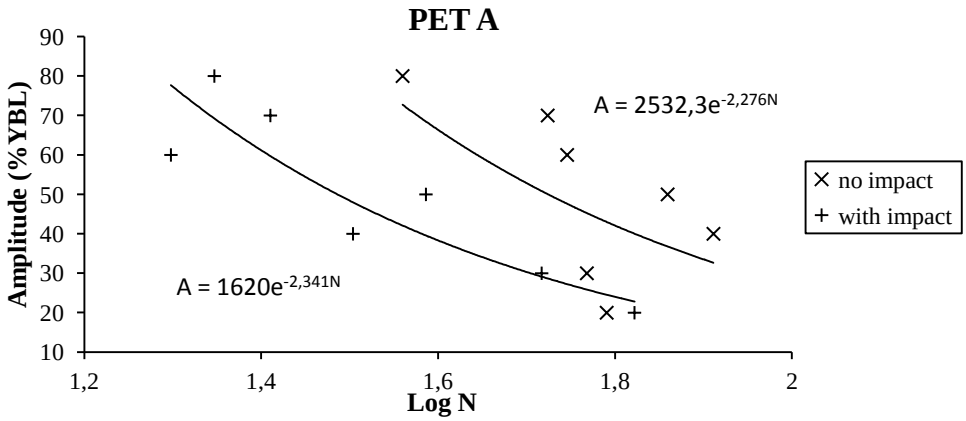

Figure 6. Cycles up to failure versus loading amplitude for different samples of PET A: virgin and damaged by the impact test

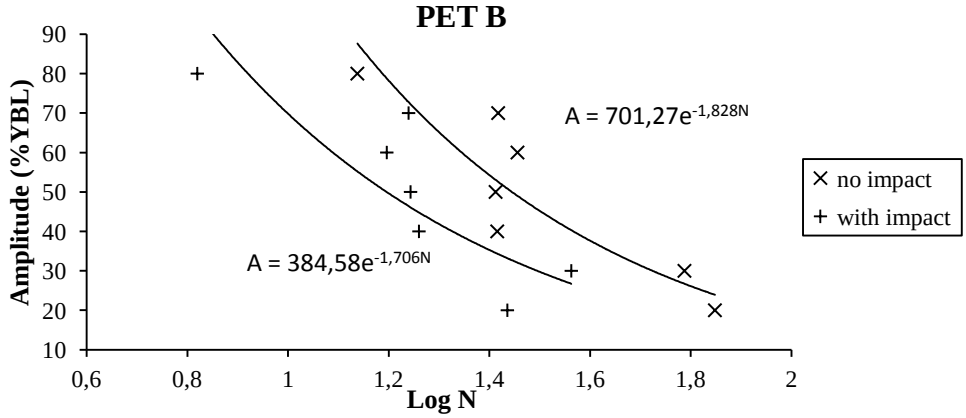

Figure 7. Cycles up to failure versus loading amplitude for different samples of PET B: virgin and damaged by the impact test

Bosman (1996) discussed the significant reduction in the number of cycles until the rupture on the ropes of polyester when submitted to cyclic loading with a high maximum tension and Banfield et al. (1999) suggested as an alternative, to reduce the duration of the fatigue testing, applies extremely conditions of loading. So, it was found that the fatigue tests didn't exceed 45 minutes, and both PET A and PET B, virgin and damaged by the impact test, have a behavior tendency of their fatigue resistance increasing as the loading amplitude decreases in load range with a inferior force high, as shown in Fig. 6, 7.

4.2. Effect of an impact test on polyester multifilaments

Table 1 shows the average, maximum and viscoplastic deformations, measured by a scale in the course of the impact tests. The elastic deformation and stored energy, are calculated from Eq. (8), (10).

Table 1. Physical Parameters

Material	PET A	PET B
Maximum Deformation (m)	0,045	0,048
Viscoplastic Deformation (m)	0,013	0,012
Elastic Deformation (m)	0,032	0,037
Stored Energy (J)	5,144	5,383

Nikonov *et al*, (2011) detected, while studying the maximum elongation of wet and dried polyamide ropes, that wet ropes tend to develop larger tensile forces and elongations then the dried ones. The device used in the present paper does not allow the measurement of force, however, in terms of elongation, it was observed that PET B has shown a higher deformation among the materials tested. The viscoplastic deformation was found to be the largest in PET A, even though the difference to PET B is considered to be quite low. PET B was the material that showed the largest elastic deformation. The elastic part of the deformation is known to be responsible for pulling back the specimen vertically after the impact, generating high amounts of deceleration and acceleration, which can be considered to be undesirable. Nikonov *et al*, (2011) have also identified that wet specimens store higher amounts of elastic energy due to higher elongations, which was also identified in this paper for PET B.

All the materials were submitted to previous impact tests and it was verified that a mass equivalent to 13% of the material's YBL, when dropped from 300 mm height is sufficient to lead to the failure of PET A and PET B. In addition, some samples were analyzed in SEM (Scanning Electron Microscopy), located in the Centro de Microscopia Eletrônica da Zona Sul - FURG, which showed the filament fractures (Fig. 8) of PET C.

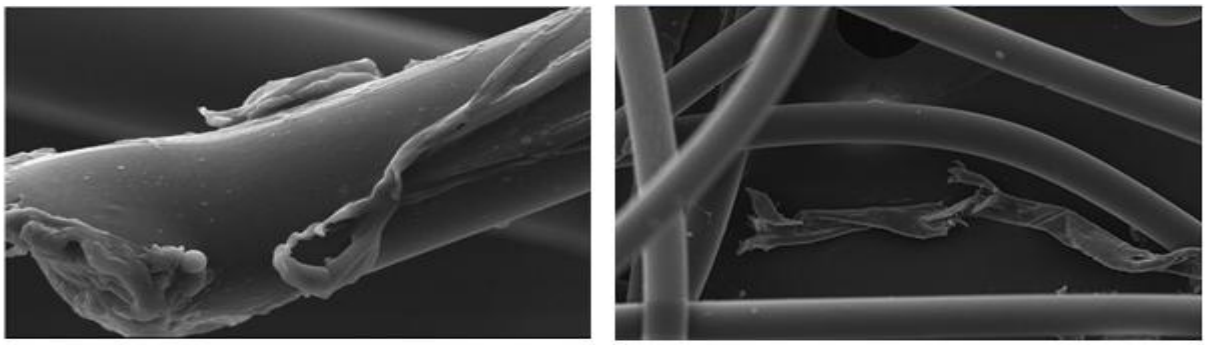

Figure 8. Filaments ruptured after impact test

5. CONCLUSIONS

The present work showed an evaluation of the fatigue behavior of different PET specimens, both in their virgin state or being previously submitted to sudden tensile loads, and discussed the effects of parameters such as material and load level over the fatigue life of each specimen. It was clearly showed that a higher tensile strength is not related to a higher fatigue resistance: PET A is the material with the lowest YBL and preformed then PET B for all the load ranges tested (Fig. 5 – PET X – with impact). In all cases, the materials suffered a drop in their fatigue life when one compares data without and with a previous impact load of 13% of their YBL.

It can be suggested the investigation of the effects of lower impact loads over the fatigue behavior of polyester yarns in future research.

Regarding the investigated parameters in the impact tests, a higher elasticity, greater absorbed energy and greater elongation of the PET B material is verified, however, it is necessary to investigate others parameters, such as the dissipated energy, for an evaluation of the quality of each material during a sudden load. This others parameters will be addressed in a future paper.

6. REFERENCES

Banfield, Stephen J., et al. "Comparison of fatigue data for polyester and wire ropes relevant to deepwater moorings." 18th International Conference on Offshore Mechanics and Arctic Engineering Proceedings. 1999.

Barbetta, Pedro Alberto, Marcelo Menezes Reis, and Antonio Cezar Bornia. Estatística: para cursos de engenharia e informática. Vol. 3. São Paulo: Atlas, 2004.

Bosman, Rig0 LM. On the origin of heat build-up in polyester ropes. In: OCEANS'96. MTS/IEEE. Prospects for the 21st Century. Conference Proceedings. IEEE, 1996. p. 332-338.

Custer, Dave. "An estimation of the load rate imparted to a climbing anchor during fall arrest." The Engineering of Sport 6 (2006): 45-50.

Emri, Igor, et al. "Time-dependent behavior of ropes under impact loading: A dynamic analysis." Sports Technology 1.4-5 (2008): 208-219.

da Costa Mattos, H. S., and F. E. G. Chimisso. "Modelling creep tests in HMPE fibres used in ultra-deep-sea mooring ropes." International Journal of Solids and Structures 48.1 (2011): 144-152.

de Camargo, Felipe Vannucchi, et al. "Cyclic stress analysis of polyester, aramid, polyethylene and liquid crystal polymer yarns." Acta Polytechnica56.5 (2016): 402-408.

Hage Jr, Elias. "Aspectos Históricos sobre o Desenvolvimento da Ciência e da Tecnologia de Polímeros." Polímeros 8.2 (1998): 6-9.

Louzada, Emilio Luiz Vieira, Carlos Eduardo Marcos Guilherme, and Felipe Tempel Stumpf. "EVALUATION OF THE FATIGUE RESPONSE OF POLYESTER YARNS AFTER THE APPLICATION OF ABRUPT TENSION LOADS." Acta Polytechnica CTU Proceedings 7 (2016): 76-78.

Marôco, João. Análise estatística com o SPSS Statistics. ReportNumber, Lda, 2011.

Martin, D. A., et al. "An approach for quantifying dynamic properties and simulated deployment loading of fire service escape rope systems." Experimental Techniques (2014).

McLaren, A. J. "Design and performance of ropes for climbing and sailing." Proceedings of the Institution of Mechanical Engineers, Part L: Journal of Materials: Design and Applications 220.1 (2006): 1-12.

McKenna, Henry A., John WS Hearle, and Nick O'Hear. Handbook of fibre rope technology. Elsevier, 2004.

Nikonov, A., et al. "Influence of moisture on functional properties of climbing ropes." International Journal of Impact Engineering 38.11 (2011): 900-909.

Pfarrius, J. D., E. Duarte, and F. E. G. Chimisso. "Theoretical and experimental modeling of a socket sandwich for use in tension tests of synthetic ropes." Vrnjacka Banja: 6th Youth Symposium on Experimental Solid Mechanics. 2007.

Smith, R. A. "The development of equipment to reduce risk in rock climbing." Sports Engineering 1.1 (1998): 27-39.

Pavier, Martyn. "Experimental and theoretical simulations of climbing falls." Sports Engineering 1.2 (1998): 79-91.

Vogwell, Jeffrey, and J. M. Minguez. "The safety of rock climbing protection devices under falling loads." Engineering Failure Analysis 14.6 (2007): 1114-1123.

WANG, Fei; HUANG, Guo-liang; DENG, De-heng. Steady state analysis of towed marine cables. Journal of Shanghai Jiaotong University (Science), v. 13, n. 2, p. 239-244, 2008..

Wang, Wenkai, Xuefeng Wang, and Guoliang Yu. "Penetration depth of torpedo anchor in cohesive soil by free fall." Ocean Engineering 116 (2016): 286-294.

7. RESPONSIBILITY NOTICE

The authors are the only responsible for the printed material included in this paper.